Journal of Intelligent Systems and Control
https://www.acadlore.com/journals/JISC

Optimization of Lateral Transfer Inventory of Auto Spare Parts Based on Neural Network Forecasting

Xinhao Shao, Daofang Chang*, Meijia Li

School of Logistics Engineering, Shanghai Maritime University, 200000 Shanghai, China

* Correspondence: Daofang Chang (dfchang@shmtu.edu.cn)

Received: 06-25-2022 **Revised:** 07-26-2022 **Accepted:** 08-12-2022

Citation: X. H. Shao, D. F. Chang, and M. J. Li, "Optimization of lateral transfer inventory of auto spare parts based on neural network forecasting," *J. Intelli Syst. Control*, vol. 1, no. 1, pp. 2-17, 2022. https://doi.org/10.56578/jisc010102.

Abstract: Creating a fair replenishment strategy is one of the most significant instruments in the inventory management for automotive spare parts. It is also crucial to controlling the enterprise's inventory level. This study considers the significance of retailers' demand forecasting at the conclusion of the sales period to build a lateral transfer inventory optimization scheme with high scientific rigor, aiming to ensure the correctness and logic of the replenishment strategy. To provide a more scientific direction for the inventory management of an automotive spare parts company, this research constructs an upgraded particle swarm optimization (PSO)-backpropagation (BP) neural network prediction model, and a lateral transfer inventory optimization method based on demand forecasting. Finally, 26 retailers of Company B in Central China's Hunan Province were taken as examples to confirm the model's efficacy. The outcomes demonstrate an improvement in the lateral transfer's applicability in Company B.

Keywords: Inventory optimization; Lateral transfer; Demand forecasting; Classification of automotive spare parts

1. Introduction

With the yearly growth in car ownership in China, the automotive aftermarket spare parts market has exhibited a positive development trend [1, 2]. The National Bureau of Statistics of China reports that vehicle spare parts businesses have enormous inventories and that managing those inventories has become exceedingly challenging. Therefore, a major concern in the automotive spare parts business is the scientific development of the replenishment strategy for spare parts products, the acceptable allocation and effective supply of inventory resources, and the improvement of the replenishment efficiency of companies.

This study proposes a multi-criteria spare parts classification strategy based on data analysis for the features of automotive spare parts. Drawing on the classification outcomes, a neural network-based spare parts supply demand prediction model was proposed to accurately predict the demand quantity of retailers at the end of the sales period. The predicted demand quantity is employed as the parameter input, and the demand satisfaction rate is taken as the output parameter. Finally, the authors developed the best inventory management plan based on the application of the lateral transfer technique.

2. Background

The inventory of automotive spare parts faces a number of problems, such as low retailer participation in the early stages of new product launch, ineffective information transfer among supply chain participants, slow supply chain response, lack of an effective inventory management mechanism, and unbalanced inventory [3]. This research uses the lateral transfer technique to acquire an inventory management solution with high scientificity by applying it to the everyday inventory management process of automobile spare parts companies.

Given the aforementioned problems, this paper develops an improved PSO-BP neural network prediction model, and devises a lateral transfer inventory optimization strategy based on demand forecasting, in the light of the complexity and rationality of transfer decisions. The purpose is to adjust the unbalanced inventory at the sales

terminal, lower the likelihood of inventory backlog and out-of-stock rate, and improve the response time. Figure 1 depicts the technical flow of this research.

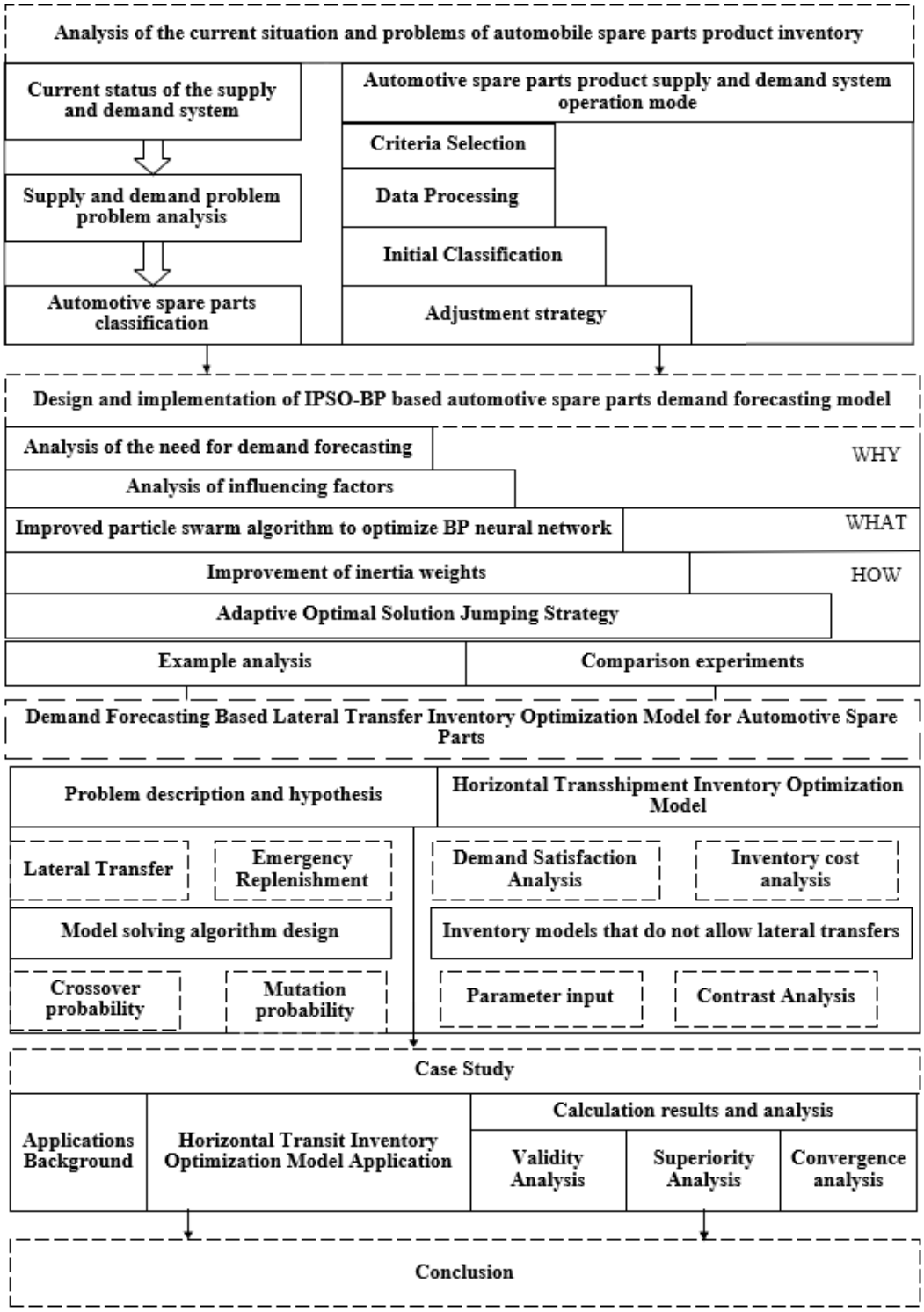

Figure 1. Technology route

3. Cluster-Based Classification

When different types of spare parts are categorized by simply taking into account one indicator of capital ownership, companies experience low inventory turnover, significant inventory backlogs, and the unavailability of some spare parts to satisfy consumer needs because they are out-of-stock [4-8]. As shown in Figure 2, this research suggests a cluster analysis-based strategy for classifying automotive spare parts.

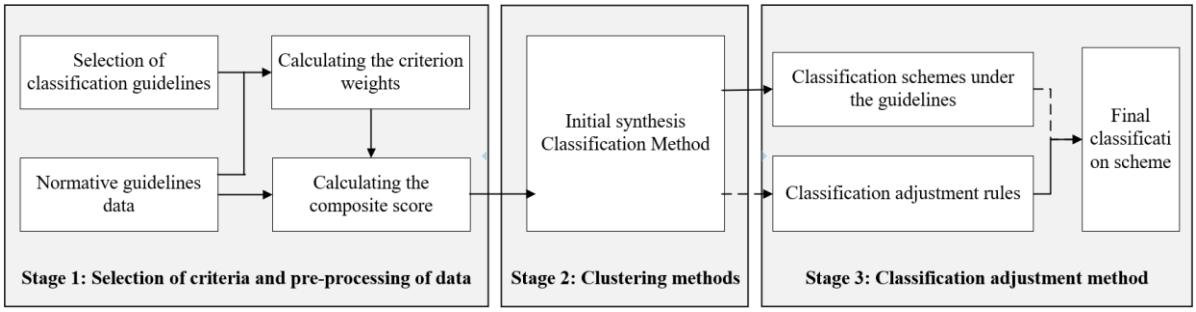

Figure 2. Framework of our classification method

3.1 Phase 1: Preliminary Data Processing

This phase primarily consists of two steps: selecting classification criteria, and data analysis and processing. Firstly, identify the spare parts to be classified m∈M, and select multidimensional classification criteria n∈N. Then, preprocess the data for the spare parts under each criterion x_{mn} (m∈M, n∈N), get normalized data x*mn, and weigh each criterion w_n (n∈N), and obtain the combined score of spare parts Q_m.

(1) Data normalization

The number of spare parts m differs with the criteria. Some data are of the positive type and some are of the negative type. The difference may affect the classification effect [9]. To eliminate the difference and obtain x_{mn} and x^*_{mn}, the revenue-based criterion and the cost-based criterion can be respectively processed by:

$$x_{mn} = \frac{x_{mn} - \min_{m=1,2,3\ldots M} x_{mn}}{\max_{m=1,2,3\ldots M} X_{mn} - \min_{m=1,2,3\ldots M} x_{mn}} \tag{1}$$

$$x_{mn} = \frac{\min_{m=1,2,3\ldots M} x_{mn} - x_{mn}}{\max_{m=1,2,3\ldots M} X_{mn} - \min_{m=1,2,3\ldots M} x_{mn}} \tag{2}$$

(2) Calculating the combined score

The weight of each criterion w_n is obtained through analytical hierarchy process (AHP), based on the survey results on the relevant personnel of the case company [10, 11]. Then, the combined score Q_m of each spare part m can be calculated by:

$$Q_m = \sum_{n=1}^{N} w_n \times x^*_{mn} \qquad \forall m \in M \tag{3}$$

3.2 Phase 2: Initial Classification

In this phase, K-means clustering (KMC) is adopted to classify the spare parts, including determining the classification level k∈K and deriving the integrated classification results of spare parts under multiple criteria P_k (k∈K) [12, 13]. Firstly, each part is assigned to the closest class randomly, such that the Euclidean distance of spare parts in each class is the farthest from the corresponding class center:

$$SD(P_k) = \sum_{Q_m \in P_k} \left\| Q_m - \sigma_k \right\|^2 \tag{4}$$

where, $\sigma^{\hat{k}}$ denotes the class center of the k-th class; SD($P^{\hat{k}}$) is the sum of the distances from the spare parts in the k-th class to the corresponding class center.

Next, the total Euclidean distance of spare parts in all classes to the corresponding class centers can be calculated by:

$$SD(\overline{Q_m}) = \sum_{k=1}^{K} \sum_{Q_m \in P_k} \left\| Q_m - \sigma_k \right\|^2 \tag{5}$$

Further, the contour coefficient (SC) is introduced to evaluate the clustering effect. The contour coefficient S(m) can be calculated by:

$$S(m) = \frac{\beta(m) - \alpha(m)}{\max[\alpha(m), \beta(m)]} \tag{6}$$

where, $\alpha(m)$ is the mean distance from spare part m to other spare parts in the same class; $\beta(m)$ is the mean distance from spare part m to spare parts in another class. Eq. (6) suggests that the contour coefficient $S(m) \in [-1,1]$. The essence of the coefficient is to solve the maximum mean distance from a spare part to spare parts in another class, and the relative error of the mean distance from the spare part to the other spare parts in the same class. $\alpha(m)$ and $\beta(m)$ reflect the cohesiveness and separation of the classes, respectively.

3.3 Phase 3: Veto-Based Class Adjustment

The KMC is applied to determine the classes of spare parts under each criterion, aiming to overcome the defects of compensatory multi-criteria classification results $P_{kn}(k \in K, n \in N)$. On this basis, the initial classes are adjusted properly to finalize the classes. After the adjustment, an arithmetic analysis is performed on M=30 spare parts of a company. The number of classes K was set to 3, and four criteria were selected, including replacement cycle, sales, unit price, and criticality. The classification results are displayed in Table 1.

Table 1. Classification results of cluster-based classification and adjustment

Serial number	Replacement cycle		Sales		Unit price	
	Numerical value	Class	Numerical value	Class	Numerical value	Class
1	0.96	A	0.09	C	0.04	C
2	0.97	A	0.54	B	0.01	C
3	0.89	A	0.2	B	0.24	B
4	0.74	A	0.28	B	0.16	B
5	0.6	B	0.07	C	0.02	C
6	0.72	B	0.08	C	0.21	B
...	...	...	...	...	...	...
27	0.57	B	0.26	B	0.17	B
28	0.24	C	0.43	B	0.06	C
29	0.2	C	0.01	C	0.01	C
30	0.63	B	0.2	B	0.21	B

Serial number	Replacement cycle		Sales		Original class
	Numerical value	Class	Numerical value	Class	
1	0.45	B	0.365	B	C
2	0.45	B	0.519	A	B
3	1	A	0.584	A	B
4	0.45	B	0.405	B	A
5	0	C	0.142	C	B
6	0	C	0.204	C	C
...	...	...	...	...	...
27	1	A	0.531	A	B
28	0.45	B	0.343	B	C
29	0	C	0.045	C	C
30	1	A	0.528	A	B

4. Improved PSO-BP Forecasting Model

4.1 Selecting Influencing Factors

Referring to the offline research of several spare parts companies, this paper analyzes and organizes the factors that influence the demand forecast of retailers of automotive spare parts, respectively from the angle of suppliers and retailers.

4.2 Demand Forecasting Model and Algorithm

Although BP neural networks are frequently employed for prediction tasks, they have disadvantages like sluggish convergence, numerous iterations, a propensity for local optimums, and limited global search capabilities. The PSO is used to optimize the connection weights and thresholds of the neural network because this swarm intelligence optimization algorithm has a great global search ability in the early stages of solving complicated problems.

The parameters of the BP neural network are defined in this work using a three-layer topology, as given in Table 2. Tanh is selected as the neural network's activation function:

$$f(z) = Tanh(z) = \frac{e^{z} - e^{-z}}{e^{z} + e^{-z}} \tag{7}$$

Table 2. Parameters of BP neural network

Name	Meaning
i=1, 2, ..., I	Number of input layer nodes
η=1, 2, ..., K	Number of data pairs
X^{η}={x_1^{η}, x_2^{η}, ..., x_I^{η}}	Input vector
l=1, 2, ..., L	Number of hidden layer nodes
Ma^{η}={ma_1^{η}, ma_2^{η}, ..., ma_L^{η}}	Input vector of hidden layer
Mb^{η}={mb_1^{η}, mb_2^{η}, ..., mb_L^{η}}	Output vector of hidden layer
α_l	Threshold of hidden layer nodes
W_{il}	Connection weight between input layer and hidden layer
Y^{η}={y_1^{η}, y_2^{η}, ..., y_J^{η}}	Vector of expected outputs
j =1, 2, ..., J	Number of output layer nodes
Na^{η}={na_1^{η}, na_2^{η}, ..., na_J^{η}}	Input vector of output layer
Nb^{η}={nb_1^{η}, nb_2^{η}, ..., nb_J^{η}}	Output vector of output layer
β_j	Threshold of output layer nodes
W_{lj}	Connection weight between hidden layer and output layer
λ	Number of iterations

The error function is defined as the deviation between the actual and expected outputs for each data pair from the training set of the BP neural network:

$$E_{\eta} = \frac{1}{J}\sum_{j=1}^{J}(y_j^{\eta} - nb_j^{\eta})^2 \tag{8}$$

The total error for all data pairs can be calculated by:

$$E = \sum_{\eta=1}^{K} E_{\eta} = \frac{1}{KJ}\sum_{\eta=1}^{K}\sum_{j=1}^{J}(y_j^{\eta} - nb_c^{\eta})^2 \tag{9}$$

The input and output of each hidden layer node can be respectively calculated by:

$$ma_l^{\eta} = \sum_{i=1}^{I} W_{il} \cdot x_i^{\eta} - \alpha_l \tag{10}$$

$$mb_l^{\eta} = f(ma_l^{\eta}) \tag{11}$$

The input and output of each output layer node can be respectively calculated by:

$$na_j^{\eta} = \sum_{l=1}^{L} W_{lj} \cdot mb_l^{\eta} - \alpha_j \tag{12}$$

$$nb_j^{\eta} = f(na_j^{\eta}) \tag{13}$$

4.3 PSO Improvement

Suppose there are P particles in the D-dimensional target search space. The position and velocity of a particle are denoted by x and v, respectively. Then, the particle is affected by the three components in Figure 3. This study tries to improve the inertia weights and adaptive optimal solution jumping strategy for the PSO algorithm [14].

(1) Improving inertia weights

In the initial search phase, the inertia weights are is reduced nonlinearly using a function, which enhances the ability for global search and speeds up the start of the local search. After several iterations, the inertia weights begin to decline linearly. Then, the algorithm can stably converge to the optimal solution. The PSO algorithm is therefore improved.

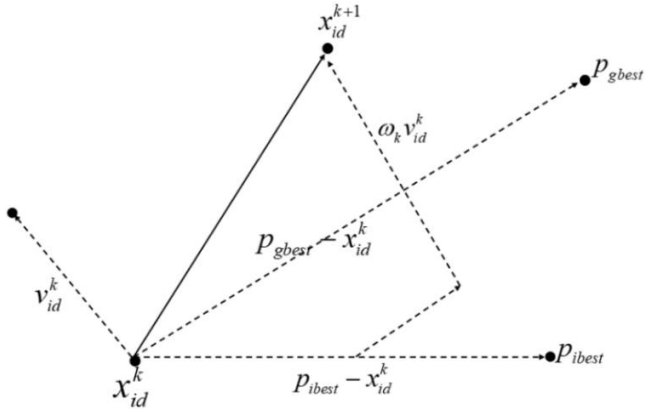

Figure 3. Motion trajectory of particles in PSO

The inertia weight functions can be expressed as:

$$\omega(k) = \begin{cases} \omega_{\min} + (\omega_{\max} - \omega_{\min}) \times s_1(k), k < L \\ \omega_{\max} - (\omega_c - \omega_{\min}) \times s_2(k), k \geq L \end{cases} \tag{14}$$

$$s_1(k) = \frac{1}{1 + e^{-(k/K)}} \tag{15}$$

$$s_2(k) = -\frac{2k}{K} \tag{16}$$

where, k is the current number of iterations; K is the maximum number of iterations; ω_{max} and ω_{min} are the maximum and minimum inertia weights, respectively; $s_1(k)$ is a nonlinear function; $s_2(k)$ is a linear function; ω_c is the initial inertia weight after a particle completes the search.

(2) Adaptive optimal solution jumping strategy

Referring to the mutation operation of the genetic algorithm (GA), the mutation factor is introduced to adjust the position of particles to enter other regions to continue with the search. In this way, the particles will not easily fall into the local optimum trap, and the algorithm can find the global optimal solution with a greater probability. The mutation operation can be expressed as:

$$x_i^t = x_i^t + s \tag{17}$$

where, t is the number of iteration falling into the local optimum trap; s is the regulated search length:

$$s = \frac{u}{|v|^{\frac{1}{\beta}}} \tag{18}$$

where, $u(0,\sigma_u^2)$ and $v(0,1)$ are equal to 0. The variance can be calculated by:

$$\sigma_u = \left\{ \frac{\phi(1+\beta)\sin(\frac{\beta\pi}{2})}{\phi(\frac{1+\beta}{2})\beta^{2(\frac{\beta-1}{2})}} \right\}^{\frac{1}{\beta}}, \sigma_v = 1 \tag{19}$$

where, $\phi(x) = \int_0^\infty t^{x-1}e^{-1}dt$.

During the position update of particles, the alternation between long and short intervals benefits the algorithm, and helps to avoid the local optimum trap and expand the entire search space.

4.4 Algorithm Design

The PSO was combined by the above two improvements to produce the improved PSO (IPSO) below.

Algorithm IPSO

Train (XT)

Input population size P; particle dimension D; maximum number of iterations K; initial particle position X_{id}; initial particle velocity V_{id}; initial inertia weights ω; initial local optimal solution P_{ibest}; initial global optimal solution P_{gbest}.

for $k \leq K$ do

update the inertia weight by Eq. (14) and update x_i by Eq. (16)

initialize the P_{ibest} and P_{gbest}

calculate the fitness of each new particle

if $f(x_i) f(P_{ibest})$ do

$P_{ibest}=x_i$

end if

if $f(P_{ibest}) f(P_{gbest})$ do

$P_{gbest}=P_{ibest}$

end if

update the position of x_i

$k=k+1$

endfor

Output Optimal particle position and particle velocity

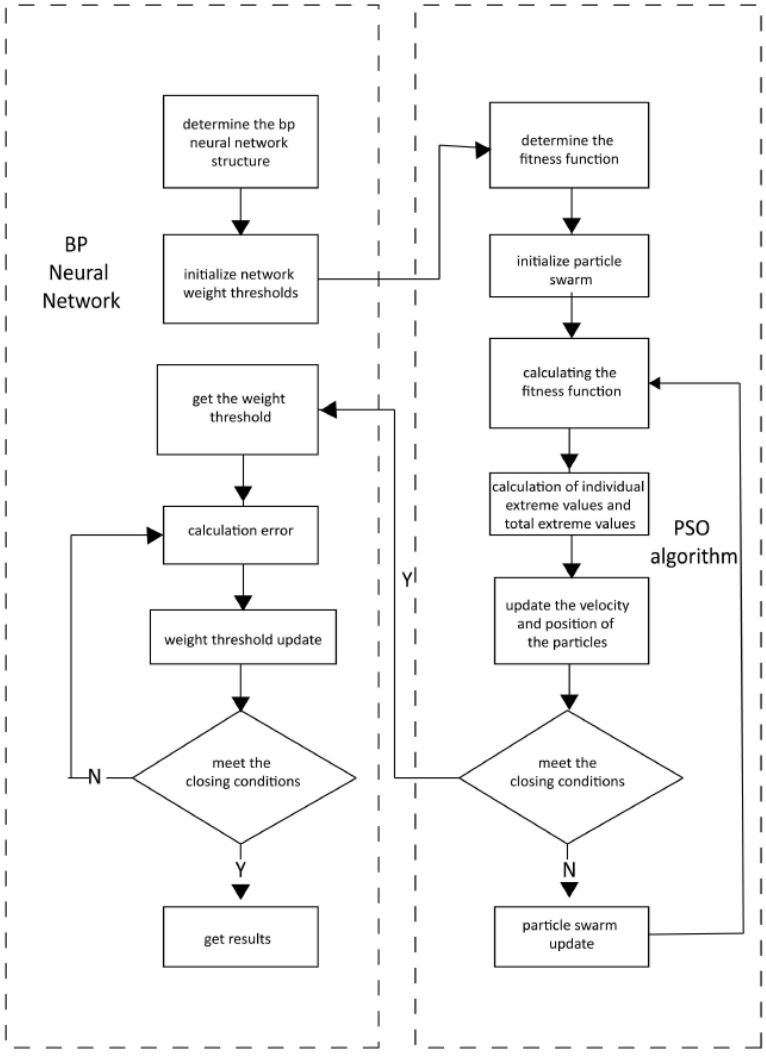

Figure 4. Flow of IPSO-BP neural network

The connection weights and thresholds of the BP neural network are optimized using the IPSO in conjunction with the foregoing construction and description of the BP neural network to address the issue that the BP neural network is sensitive to the connection weights and thresholds. The flow chart of the optimization algorithm is shown in Figure 4.

The IPSO optimizes the BP neural network in the following manner:

Step 1: Based on the training samples, determine the architecture of the BP neural network. Next, initialize the connection weights and thresholds of the network with random numbers [0, 1].

Step 2. The population and dimension of the particle swarm method are combined with the structure of the BP neural network, and the initial position and velocity of each particle are set in accordance with the connection weights and thresholds initialized by the BP neural network.

Step 3. Select any pair, $X^{\eta}=\{x_1^{\eta}, x_2^{\eta}, ..., x_I^{\eta}\}$ and $Y^{\eta}=\{y_1^{\eta}, y_2^{\eta}, ..., y_J^{\eta}\}$ from the training samples.

Step 4. Calculate the output of hidden layer nodes, and the output of output layer nodes.

Step 5. Run the IPSO, set the fitness function, and calculate the fitness value, i.e., the error. Then, take the error as the termination condition for IPSO operation. If the error is below the set value, terminate the optimization, output the velocity and position of the particles, and enter the next step. Otherwise, continue with the optimization by the IPSO until the error falls below the set value, or the maximum number of iterations is reached.

Step 6. Assign the resulting velocity and position of the particles to the BP neural network, serving as the optimal connection weights and thresholds.

Step 7. Determine whether all the samples in the training set have completed training. If yes, go to Step 8. Otherwise, take the current successive weights and thresholds of the BP neural network as the initial velocity and position of the IPSO, and return to Step 3 for further training.

Step 8. Calculate the total error of all training samples, and terminate the training based on whether the total error is less than the set value. If the termination condition is satisfied, the training is complete. Otherwise, take the updated connection weights and thresholds of the current BP neural network as the initial speed and position of the IPSO, and return to Step 3 to continue with the training, until reaching the termination condition.

4.5 Example Analysis

The example analysis targets a retailer in a company's regional center. The authors collected inventory data for a brand of general-purpose wiper blades made by the company, and divided the samples into a training set and a test set. The training samples are used to correct weights and parameters for network training, while the test samples determine whether the network is stable and meets the requirements. Table 3 displays the parameters of the IPSO-BP neural network prediction model utilized in the case.

Table 3. Model design

Parameter name	Parameter value
Number of input layer nodes	8
Number of output layer nodes	1
Number of hidden layers	1
Number of hidden layer nodes	10
Activation function of input layer to hidden layer	tanh
Activation function of hidden layer to output layer	purelin
Learning function	learngdm
Training function	trainlm
Data normalization function	$x_{norm}=\frac{x-x_{\min}}{x_{\max}-x_{\min}}$
Mean squared error	$MSE=\frac{1}{N}\sum_{n=1}^{N}(f(x_i)-y_i)^2$
Standard deviation	$SD=\sqrt{\frac{1}{N}\sum_{n=1}^{N}(f(x_i)-\mu)^2}$

Compared with the traditional PSO-BP model, the IPSO-BP model includes the adaptive optimal solution jumping strategy and improved inertia weights. To verify its prediction accuracy and stability, the IPSO-BP was compared with three relevant models: BP model, PSO-BP model, and GA-BP model. The four models were run 20 times independently on the test dataset. The results of these models are compared in Figure 5 and Figure 6.

As shown in Figure 5, IPSO-BP and PSO-BP converged faster and more accurately than the other two models. Meanwhile, IPSO-BP, thanks to PSO improvement, could search through more space in the first iteration. This ensures the stable convergence to the global optimal solution, and the accuracy of local search. As shown in Figure 6, IPSO-BP ended up with fewer prediction errors during sample testing.

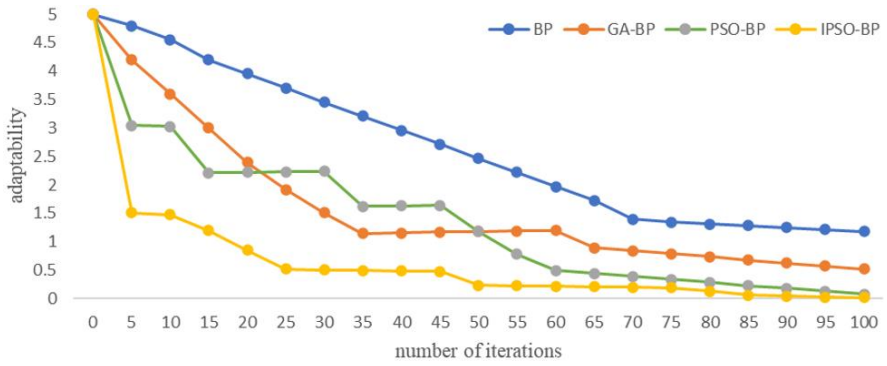

Figure 5. Fitness of different models

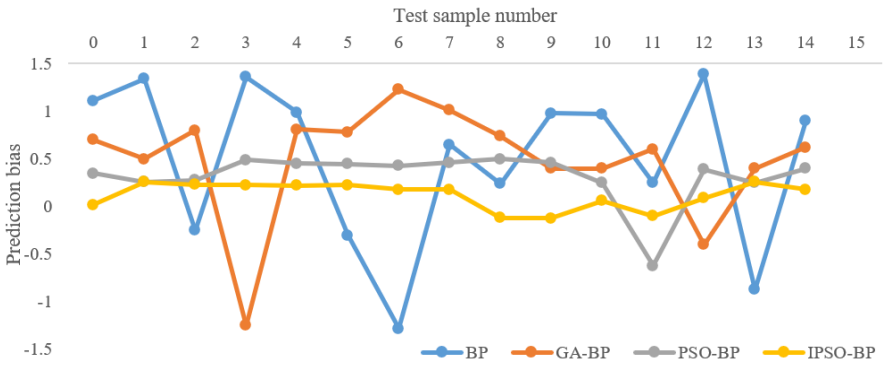

Figure 6. Prediction errors of different models

5. Optimization Model

5.1 Problem Description

In this section, a lateral transfer inventory optimization system is created for a regional center and several retailers. As sales increase after the company's first distribution is complete, certain retailers' inventories reach a critical point where they are unable to meet customer demand, creating a critical shortage of products [15-19]. The lateral transfer strategy is thus activated in the system.

5.2 Symbols and Parameters

Table 4 lists the model symbols and their definitions.

Table 4. Symbols and definitions

Symbols	Definition
K	Retailer set $K = \{1, 2, ..., k\}$and $i,j \in K$
D_i	End-of-period spare parts demand of retailer i
Q_{ij}	Number of transits for lateral transfers
Si	Emergency replenishment volume of the regional center
I_i	Inventory of retailer i during the launch period of new products
N_i	Current inventory of retailer i
V_i	Maximum storage capacity of retailer i
x_{ij}	0-1 variable about whether lateral transfer occurs
f	Overall demand fulfillment of the regional center
α	Limitation of overall product demand rate of the regional center
c_1	Inventory holding cost per unit of spare parts
c_2	Lateral transfer cost per unit of spare parts
c_3	Emergency replenishment costs per unit of spare parts of the regional center
c_4	Out-of-stock cost per unit of spare parts
C_H	Inventory holding costs in lateral transfers
C_T	Lateral transfer costs
C_z	Fixed costs of lateral transfer
C_B	Out-of-stock costs in lateral transfer
C_z	Emergency transaction costs

5.3 Optimization Model

The demand fulfilment rate of the regional center can be expressed as [8]:

$$f = \sum_{i=1}^{K}[(N_i + S_i + \sum_{j=1, j\neq i}^{K} x_{ij}Q_{ij}) / D_i] \tag{20}$$

The inventory holding, lateral transfer, out-of-stock, and emergency replenishment costs of the regional center can be respectively calculated by:

$$C_H = c_1 \cdot \sum_{i=1}^{K}(N_i + \sum_{j=1, j\neq i}^{K} x_{ij}Q_{ij} - D_i) \tag{21}$$

$$C_T = c_2 \cdot \sum_{i=1}^{K}(\sum_{j=1, j\neq i}^{K} x_{ij}Q_{ij}) + C_z \tag{22}$$

$$C_B = c_4 \cdot \sum_{i=1}^{K}(D_i - N_i - \sum_{j=1, j\neq i}^{K} x_{ij}Q_{ij} - S_i) \tag{23}$$

$$C_s = \sum_{i=1}^{K} c_3 \cdot S_i \tag{24}$$

5.4 Model Building

After the lateral transfer, the total operation cost of the regional center can be minimized by:

$$\min TC_1 = \min(C_H + C_T + C_B + C_S) \tag{25}$$

The lower bound for maximizing the overall satisfaction rate of product demand of the regional center can be determined by:

$$\max TC_2 = \min f_i \tag{26}$$

The out-of-stock retailer cannot receive more than its forecasted demand for spare parts:

$$\sum_{j=1}^{K} x_{ij} \cdot Q_{ij} \leq D_i + r_i - N_i \tag{27}$$

The demand and received inventory of retailer i cannot exceed its maximum inventory capacity:

$$\sum_{j=1}^{K} x_{ij} \cdot Q_{ij} + N_i \leq V_i \tag{28}$$

If a replenishment retailer meets its own demand and maintains its inventory level, it can transfer the following quantity to the out-of-stock side:

$$\sum_{i=1}^{K} x_{ij} \cdot Q_{ij} \leq N_j - D_j - r_j \tag{29}$$

The supply from a replenishment retailer to the out-of-stock side needs to meet the following condition:

$$\sum_{i=1}^{K} x_{ij} \leq 1 \tag{30}$$

The number of out-of- stock retailers that can receive replenishment must be limited by:

$$\sum_{j=1,i\neq j}^{K} x_{ij} \leq K-1 \tag{31}$$

The lateral transfer volume to meet the demand of out-of-stock retailers can be determined by:

$$D_i = \sum_{j=1}^{K} x_{ij} \cdot Q_{ij} + N_i + S_i \tag{32}$$

The demand satisfaction for the regional center as a whole must be limited by:

$$f \geq \alpha \tag{33}$$

The retailers' demand must be satisfied in the following order:

$$C_H > C_T > C_B > C_S > 0 \tag{34}$$

The out-of-stock and replenishment sides can be determined by:

$$0 \leq x_{ij} + x_{ji} \leq 1 \tag{35}$$

x_{ij} must be a 0-1 variable:

$$x_{ij} \in \{0,1\} \tag{36}$$

After the lateral transfer, the quantity of emergency replenishment from the regional center *i* cannot be less than the actual demand under the demand satisfaction limit:

$$S_i \geq D_i[\alpha - (N_i + \sum_{j=1,j\neq i}^{K} x_{ij} \cdot Q_{ij}) / D_i] \tag{37}$$

The selected parameters in all equations must be all non-negative integers:

$$I_{it}, N_{it}, S_i, Q_{ij} \geq 0 \tag{38}$$

5.5 Inventory Optimization Model Without Lateral Transfer

The said lateral transfer strategy was compared with an inventory optimization model without lateral transfer [20]:

To ensure economy, the various costs of the inventory strategy must be minimized:

$$\min TC_1 = \min(C_H + C_B + C_S) \tag{39}$$

After the optimization, the lower bound of the overall demand satisfaction of the maximized regional center should satisfy:

$$\max TC_2 = \min f \tag{40}$$

The replenishment demand of the out-of-stock retailer must be fully satisfied:

$$D_i = N_i + S_i \tag{41}$$

The retailer's demand must be satisfied to the minimum level:

$$f \geq \alpha \tag{42}$$

The retailers' demand must be satisfied in the following order:

$$C_H > C_B > C_S > 0 \tag{43}$$

The quantity of emergency replenishment from the regional center i cannot be less than the actual demand under the demand satisfaction limit:

$$S_i \geq D_i[\alpha - N_i / D_i] \tag{44}$$

The selected parameters in all equations must be all non-negative integers:

$$I_i, N_i, S_i \geq 0 \tag{45}$$

6. Case Study

6.1 Overview of Company B

To increase the sales market in China, Company B is responsible of the production, sales, and after-sales support of BS brand automotive parts. However, the retailers of this company fail to implement sufficient inventory management. Thus, the problem of unbalanced inventory is evident, which has a limited positive impact on business growth.

6.2 Sample Selection

Representative and universal samples were selected to verify the superiority of the lateral transfer inventory optimization model in coordinating the inventory between suppliers of automotive spare parts in the example. The demand of all sides concerning the wiper blades of a car brand was covered in the samples.

6.3 Model Parameters

The input parameters for inventory management are 2.0, 2.5, 7.0, and 5.0 for models c1-c4, in turn. Table 5 summarizes the inventory status of each retailer.

Table 5. Inventory status of each retailer

Retailer number K	Inventory points rk	Available inventory Nk	Retailer number K	Inventory points rk	Available inventory Nk
K01	2	14	K14	2	6
K02	4	12	K15	4	9
K03	3	4	K16	5	7
K04	1	7	K17	6	3
K05	2	10	K18	4	13
K06	2	5	K19	5	11
K07	4	7	K20	2	2
K08	4	6	K21	3	9
K09	1	6	K22	2	4
K10	3	4	K23	2	12
K11	2	6	K24	4	11
K12	2	7	K25	1	2
K13	3	8	K26	3	17

6.4 Lateral Transfer Inventory Optimization

(1) Demand forecasting

The product demand of each retailer of Company B was predicted by the proposed IPSO-BP neural network, based on the sales of each retailer. The network was adopted to forecast the market demand for products the end of the sales period for 26 retailers [21, 22]. The forecasting results are listed in Table 6.

(2) Optimization decisions

Based on the forecasts by the IPSO-BP, a lateral transfer inventory optimization model was constructed for each retailer of Company B, producing a decision plan of inventory optimization for each retailer. Next, the retailer demand satisfaction limit α was set to 0.85, and the demand satisfaction of a single retailer was kept above 0.85.

On this basis, the population size was configured as 20 and the maximum number of iterations as 400. Figure 7 shows the fitness convergence curve of the model solving algorithm. The retailer's lateral transfer inventory optimization scheme is obtained as shown in Figure 8.

Table 6. Forecasting results

Retailer K	Demand Dk	Retailer K	Demand Dk
K01	8	K10	4
K02	4	K11	7
K03	7	K12	10
K04	12	K13	17
K05	6	K14	3
K06	5	K15	8
K07	13	K16	4
K08	7	K17	14
K09	6	K18	5
K19	7	K23	7
K20	6	K24	9
K21	4	K25	4
K22	5	K26	15

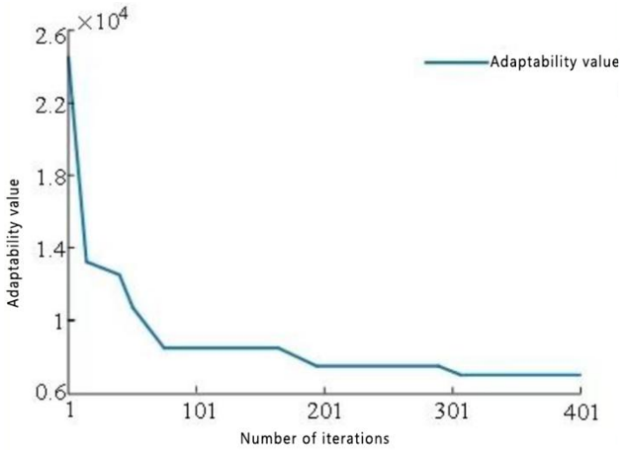

Figure 7. Convergence curve

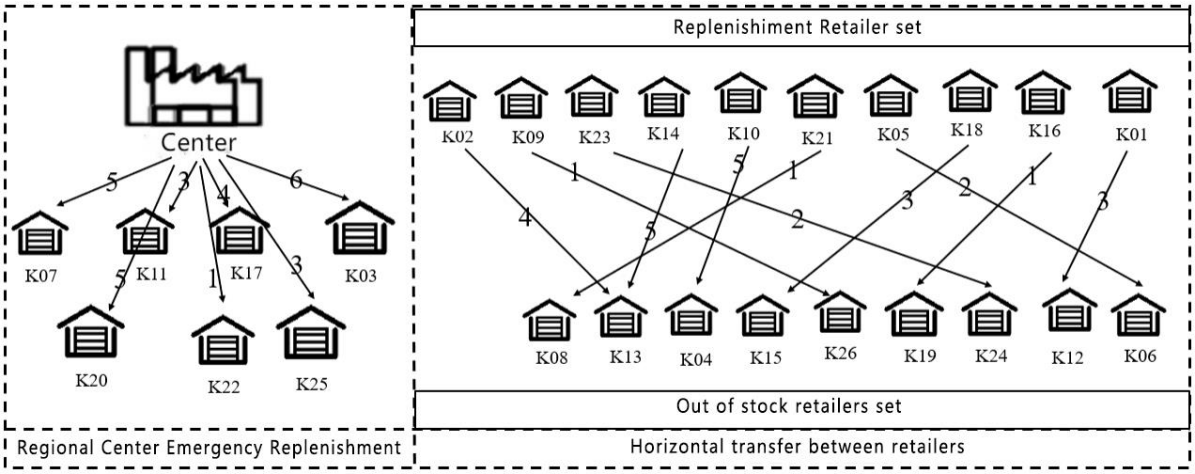

Figure 8. Lateral transfer strategy for inventory optimization based on demand forecasting

6.5 Validity Testing

(1) Validity of demand forecast

With an average increase of 60.3% in the lower bound of system demand satisfaction, our model exhibits high superiority in the control of system demand satisfaction, as shown by Table 7. The out-of-stock cost management

is impressive in terms of individual cost control, with an average reduction of up to 38.42%. The decrease in out-of-stock indirectly shows the improvement of decision fairness, which reflects the accuracy and reasonability of the plan based on the demand forecast. This is because the out-of-stock cost is positively correlated with the demand prediction. In general, the proposed lateral transfer inventory optimization model, which is based on IPSO-BP demand forecasting, is highly reasonable.

Table 7. Impact of IPSO-BP-based forecasting

Demand satisfaction limit	With or without forecasting model	Total operating costs f1				Total operating costs f1	Demand satisfaction
		Inventory holdings	Lateral transfer	Out-of-stock losses	Emergency replenishment		
0.65	Yes	59.34	109	137.28	158	463.62	0.671
	No	56.82	115.3	204.27	101.45	477.84	0.65
0.7	Yes	62.45	102.37	116.79	174.86	456.47	0.768
	No	59.64	105.57	162.98	133.53	461.73	0.724
0.85	Yes	69.41	99.73	113.39	198.56	481.09	0.872
	No	67.04	94.3	156.27	147.18	464.79	0.853
0.9	Yes	57.83	113.52	53.31	231.76	456.42	1
	No	55.6	116.46	87.65	201.74	461.45	0.951

(2) Superiority of lateral transfer strategy

As can be seen from Table 8, under the same demand satisfaction limit, the inventory optimization plan that permits lateral transfers has a lower total cost than the plan that does not [23]. On average, the cost was reduction by 63.77%. Thus, the former plan successfully lowers system operating costs and enhances the economy of inventory management.

Table 8. Impact of lateral transfers

Demand satisfaction limit	With or without forecasting model	Total operating costs f1				Total operating costs f1	Demand satisfaction
		Inventory holdings	Lateral transfer	Out-of-stock losses	Emergency replenishment		
0.65	Yes	59.33	109	137.28	158	463.61	0.671
	No	147.81	-	451.94	167.56	767.31	0.65
0.7	Yes	62.45	102.37	116.79	174.86	456.47	0.768
	No	167.39	-	432.71	185.54	785.64	0.724
0.85	Yes	69.41	99.73	113.39	198.56	481.09	0.872
	No	180.92	-	437.85	208.17	826.94	0.853
0.9	Yes	557.83	113.52	53.31	231.76	456.42	1
	No	158.96	-	436.03	233.95	828.94	0.951

(3) Analysis of algorithm convergence

With the same number of iterations and population size, Table 9 shows that the computation times of data experiments for various retailers do not differ significantly, suggesting that the method will perform better when the task size is bigger. When the initial population size is 20 and the number of iterations is 300, our method performs better in terms of computational efficiency and experimental results. As a result, the parameters for the model solution are recommended as 20 for the initial population size and 300 for the number of iterations.

Table 9. Fitness and running time of different algorithms

Population size	Number of iterations	Fitness	Running time
5	50	11657.45	5.37
10	100	10378.27	19.853
20	100	9763.48	50.729
20	300	7077.14	198.634
30	500	7535.86	368.31
50	500	7241.57	483.336
50	1000	6935.1	974.862

7. Conclusions

This paper provides the optimal replenishment system under the lateral transfer strategy, using the example of automotive spare parts. This study examines a lateral transfer inventory optimization system that consists of a regional center and various retailers. Specifically, lateral transfer refers to the inventory management strategy that

fills the inventory gaps of out-of-stock retailers with the excess inventory of neighboring retailers to satisfy their replenishment demand, without harming the regular sales of the replenishment retailers. The formulation of a lateral transfer inventory optimization model, the introduction of a new product launch period, and demand forecasts for retailers all offer scientific theoretical guidance for the creation of Company B's inventory supply program.

The lateral transfer strategy was incorporated into the supply plan of the inventory optimization model. By making this change, it is possible to decrease the overall operating costs of the inventory system, increase the economy of replenishment decisions, protect each retailer's fundamental replenishment rights, and raise the level of overall demand satisfaction among retailers in the region. When it comes to enterprise inventory management, the inclusion of lateral transfer into inventory optimization strategy can increase the overall support to distribution network, address retailer inventory imbalance, and offer scientifically sound theoretical guidance for the selection of product inventory levels for automotive spare parts.

Data Availability

The data used to support the findings of this study are available from the corresponding author upon request.

Conflict of Interest

The authors declare that they have no conflicts of interest.

References

[1] D. C. Sun, "China's auto parts development strategy and countermeasures research," MSc Dissertation, Jilin University, China, 2006.

[2] P. Zhang, X. Xu, V. Shi, and J. Zhu, "Simultaneous inventory competition and transshipment between retailers," *Int J. Prod. Econ*., vol. 230, Article ID: 107781, 2020. https://doi.org/10.1016/j.ijpe.2020.107781.

[3] P. Wan, S. F. Ji, and N. X. Song, "Multi-location inventory optimization model with lateral transshipment for random defect rate items," *Comput. Integr. Manuf. Syst*., vo. 26, no. 9, pp. 2561-2572, 2020. https://doi.org/10.13196/j.cims.2020.09.025.

[4] F. Qiao and K. Jiang, "Attitudes towards global warming on Twitter: A hedonometer-appraisal analysis," *J. Glob. Inf. Manag*., vol. 30, no. 7, Article ID: 296708, 2021. https://doi.org/10.4018/JGIM.296708.

[5] N. F. Cui and X. Luo, "ABC classification based on AHP in servicing spare part," *Ind. Eng. Manage.*, vol. 10, no. 6, pp. 33-36, 2004. https://doi.org/10.3969/j.issn.1007-5429.2004.06.008.

[6] F. Qiao and J. Williams, "Topic modelling and sentiment analysis of global warming tweets: Evidence from big data analysis," *J. Organ. End. User. Com.*, vol. 34, no. 3, Article ID: 294901, 2022. https://doi.org/10.4018/JOEUC.294901.

[7] J. Huiskonen, "Maintenance spare parts logistics: Special characteristics and strategic choices," *Int J. Prod. Econ.*, vol. 71, no. 1-3, pp. 125-133, 2001. https://doi.org/10.1016/S0925-5273(00)00112-2.

[8] M. Braglia, A. Grassi, and R. Montanari, "Multi-attribute classification method for spare parts inventory management," *J. Qual. Maint. Eng.*, vol. 10, no. 1, pp. 55-65, 2004. https://doi.org/10.1108/13552510410526875.

[9] I. Roda, M. Macchi, L. Fumagalli, and P. Viveros, "A review of multi-criteria classification of spare parts: From literature analysis to industrial evidences," *J. Manuf. Technol. Mana.,* vol. 25, no. 4, pp. 528-549, 2014. https://doi.org/10.1108/JMTM-04-2013-0038.

[10] B. E. Flores and D. C. Whybark, "Multiple criteria ABC analysis," *Int J. Oper. Prod. Man.*, vol. 6, no. 3, pp. 38-46, 1986. https://doi.org/10.1108/eb054765.

[11] R. Ramanathan, "ABC inventory classification with multiple-criteria using weighted linear optimization," *Comput. Oper. Res*., vol. 33, no. 3, pp. 695-700, 2006. https://doi.org/10.1016/j.cor.2004.07.014.

[12] F. Y. Partovi and J. Burton, "Using the analytic hierarchy process for ABC analysis," *Int J. Oper. Prod. Man.*, vol. 13, no. 9, pp. 29-44, 1993. https://doi.org/10.1108/01443579310043619.

[13] R. Ernst and M. A. Cohen, "Operations related groups (ORGs): A clustering procedure for production/inventory systems," *J. Oper. Manag.*, vol. 9, no. 4, pp. 574-598, 1990. https://doi.org/10.1016/0272-6963(90)90010-B.

[14] J. X. Chen, "Peer-estimation for multiple criteria ABC inventory classification," *Comput. Oper. Res.*, vol. 38, no. 12, pp. 1784-1791, 2011. https://doi.org/10.1016/j.cor.2011.02.015.

[15] J. Z. Sun, Y. Xu, and S. Y. Wang, "PSO with reverse edge for multi-objective software module clustering," *Int J. Perf. Eng*., vol. 14, no. 10, pp. 2423-2431, 2018. https://doi.org/10.23940/ijpe.18.10.p18.24232431.

[16] G. Y. Zhu and H. S. Yan, "A kind of demand-forecasting model based on analysis of demand booming and principle of naive forecasting," *Syst. Eng. Theor. Pract.*, vol. 24, no. 5, pp. 22-32, 2004.

https://doi.org/10.3321/j.issn:1000-6788.2004.05.004.
[17] C. L. Hu, Y. H. Liu, and J. L. Gao, "Research on prediction method of grain yield based on IPSO-BP model," *J. Chinese Agr. Mech.*, vol. 42, no. 3, pp. 136-141, 2021. https://doi.org/10.13733/j.jcam.issn.2095-5553.2021.03.019.
[18] X. L. Zhang, "Research on a three-level supply chain inventory sharing model considering transshipment strategy and demand satisfaction level constraints," MSc Dissertation, Northeastern University, China, 2015.
[19] Y. R. Zeng, L. Wang, and J. He, "A novel approach for evaluating control criticality of spare parts using fuzzy comprehensive evaluation and GRA," *Int J. Fuzzy. Syst.*, vol. 14, no. 3, pp. 392-401, 2012.
[20] Y. He, S. Y. Wang, and K. K. Lai, "An optimal production-inventory model for deteriorating items with multiple-market demand," *Eur. J. Oper. Res.*, vol. 203, no. 3, pp. 593-600, 2010. https://doi.org/10.1016/j.ejor.2009.09.003.
[21] P. Zhang, X. Xu, V. Shi, and J. Zhu, "Simultaneous inventory competition and transshipment between retailers," *Int J. Prod. Econ.*, vol. 230, Article ID: 107781, 2020. http://dx.doi.org/10.1016/j.ijpe.2020.107781.
[22] A. Bacchetti and N. Saccani, "Spare parts classification and demand forecasting for stock control: Investigating the gap between research and practice," *Omega*, vol. 40, no. 6, pp. 722-737, 2012. https://doi.org/10.1016/j.omega.2011.06.008.
[23] C. L. Hu, Y. H. Liu, and J. L. Gao, "Research on prediction method of grain yield based on IPSO-BP model," *J. Chinese Agric. Mech.*, vol. 42, no. 3, pp. 136-141, 2021. http://dx.doi.org//10.13733/j.jcam.issn.2095-5553.2021.03.019.